

1 **On the Development of a Transparent Enclosure for 360° Video Cameras to Observe**  
2 **Severe Fires In Situ**

3 Matthew S. Hoehler

4 National Institute of Standards and Technology, 100 Bureau Drive, Gaithersburg, USA,  
5 matthew.hoehler@nist.gov

6

7 **Highlights:**

- 8 • A simple and inexpensive way to significantly improve the tenability of video cameras in  
9 severe fire environments is described.
- 10 • Fabrication details required to replicate the system are provided.
- 11 • Three application cases that illustrate 360-degree video footage acquired using the system  
12 for various fire scenarios are shown to illustrate its strengths and weaknesses.

13 **Abstract:**

14 360-degree video recorded in fires provides a unique perspective that allows the viewer to  
15 change the viewing direction as regions of interest change during a fire. Use of 360-degree and  
16 traditional cameras at some locations in intense fires for extended durations has been hampered  
17 in the past by the high levels of radiant heat flux that will damage the camera's imaging sensor.  
18 This paper describes how a thin layer of moving water can be used to significantly reduce  
19 unwanted infrared radiation generated by a fire while allowing visual imaging using a simple and  
20 inexpensive enclosure. Essential details to replicate this system are provided and three  
21 illustrative example deployments are discussed.

22

23 **Keywords:** 360-degree video; fire; instrumentation; virtual reality

24

25 **1. Introduction**

26 As the saying goes, a picture is worth a thousand words.

27 Videos and images enable compelling technical storytelling and can quickly convey the  
28 significance of events and complex physical phenomena in ways that the most elegant prose or  
29 brilliantly depicted numerical data often cannot. Occasionally, images stand on their own; they  
30 are the data and the message. Frequently, images provide the context to understand the data  
31 being communicated.

32 Fire science lends itself to imaged-based data, in particular video, because it frequently deals  
33 with spatially-distributed phenomena that vary with time as a fire grows and decays. The  
34 objective of this work is twofold. First, to thermally protect cameras to allow them to record  
35 video in the middle of intense fires for indefinite durations and, second, to take advantage of  
36 recent developments in omnidirectional (360-degree) camera technologies. By using 360-degree  
37 video, as opposed to cameras with a limited directional field of view, the viewer can focus on

38 changing regions of interest and can watch video footage in immersive viewing environments  
39 such as a virtual reality head-mounted display or in room-scale virtual environments.

40 Placing cameras into fires is not new. Video and photography have long been used as primary  
41 measurement tools for fire detection [1] and in the study of flaming combustion; e.g., [2–4]. In  
42 large-scale compartment fire experiments [5–7] video is nearly always recorded and there has  
43 been widespread use of video in the study of wildland fire [8,9]. What is new about the present  
44 work is that it significantly improves the tenability of video cameras inside of severe fires in an  
45 inexpensive and robust way. In addition to resolving the obvious need to keep a camera from  
46 overheating in a fire, the solution significantly reduces the intense infrared radiation generated by  
47 the fire that would quickly damage the camera’s imaging sensor when it is close to a fire.

48 This paper describes the concept design for an enclosure to house 360-degree video cameras,  
49 provides the essential fabrication details necessary to replicate the system and shows select  
50 applications of the system that illustrate its strengths and weaknesses. This paper should be of  
51 value to fire scientists and others interested in capturing better video footage of fires.

## 52 **2. Concept design**

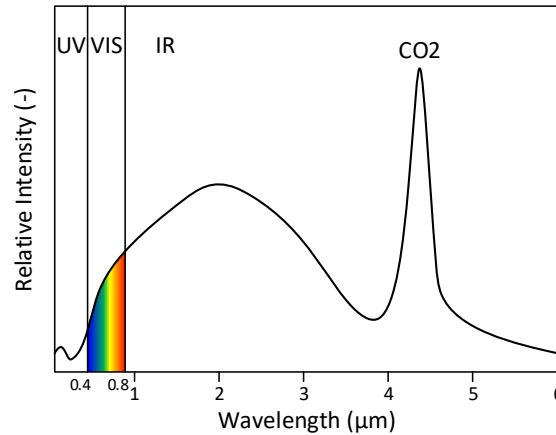
53 In fire research it is often desired to place cameras, or other optical instruments, close to a fire or  
54 another heat source (e.g., radiant panel or gas furnace) where high ambient temperatures exist. In  
55 these situations, air cooling systems or liquid (usually water) cooled metallic enclosures are often  
56 employed to protect the camera from overheating. Numerous examples of custom-built and  
57 commercially-available [10,11] systems can be found.

58 In the extreme case of a fully-developed compartment fire, however, air temperatures can exceed  
59 800 °C even near the floor of the compartment, and, more importantly, heat flux intensities  
60 inside the compartment can be greater than 150 kW/m<sup>2</sup> [12–14]. Fig. 1 shows a snapshot from  
61 video footage taken just outside of the doorway opening of a fully-developed furnished  
62 compartment fire 17 min after ignition when the heat release rate (HRR) was 10 MW. Heat  
63 fluxes measured 1.8 m above the floor along the wall of the compartment over 200 kW/m<sup>2</sup> were  
64 sustained for over 10 min [13]. For comparison, solar radiation reaching the surface of the earth  
65 on a clear day is about 1 kW/m<sup>2</sup> and heat flux of 15 kW/m<sup>2</sup> has been shown to melt a hole  
66 through polycarbonate self-contained breathing apparatus (SCBA) facepieces in less than 5 min  
67 [15]. Even if a camera is protected from overheating in such an environment, heat flux at the  
68 levels observed in a compartment fire would rapidly (in seconds) destroy the camera’s imaging  
69 sensor. Therefore, the radiant heat flux must be significantly reduced to record video.



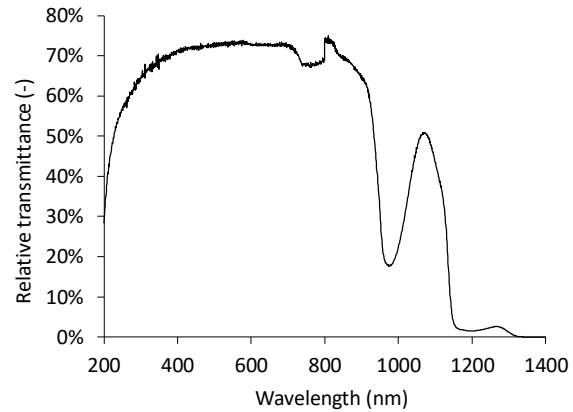
70  
71 Fig. 1. Snapshot from video footage taken outside of the doorway opening of a fully-developed  
72 furnished compartment fire extracted from [16].

73 The radiative energy produced by a hydrocarbon fire, which is often quantified in terms of heat  
 74 flux, comes primarily from spectral emissions produced by the change in energy state of  
 75 molecules during combustion, largely carbon dioxide and water, and from black-body radiation  
 76 emitted by heated soot particles. The schematic illustration in Fig. 2 emphasizes that the majority  
 77 of this radiative energy (defined as the area under the curve) is in the infrared (IR) portion of the  
 78 electromagnetic spectrum, with smaller portions in the visible (VIS) and ultraviolet (UV)  
 79 portions of the spectrum. In the case of video cameras, one wants to preserve energy at visible  
 80 wavelengths, while blocking energy at infrared (and to a small extent ultraviolet) wavelengths.



81  
 82 Fig. 2. Schematic illustration of relative intensity spectrum of a typical hydrocarbon fire.

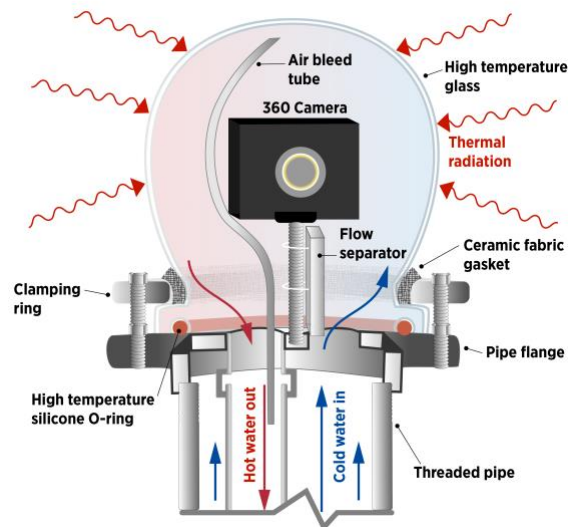
83 For low-levels of heat flux, anti-reflective (AR) coated glass filters can be used to reduce  
 84 unwanted radiant energy. However, at higher levels of heat flux, AR coated filters will not  
 85 sufficiently reduce the undesired radiation and the coatings may be prone to thermal damage.  
 86 Here, we are aided by nature. Water is extremely good at absorbing energy in the infrared  
 87 spectrum while transmitting energy in the visible spectrum. This is illustrated in Fig. 3 by a  
 88 measured transmittance spectrum for pure water. As water absorbs the energy emitted by the fire,  
 89 it is heated. The hot water can be transported away and replaced with cool water providing a  
 90 filter and heat exchanger that can survive for an indefinite time. These properties make water a  
 91 good low-pass filter for visible spectrum cameras exposed to intense fires.



92  
 93 Fig. 3. Relative transmittance spectrum for a 30 mm thick sheet of deionized water.

94 The electromagnetic radiation absorption, i.e., filtering, characteristics of liquid water can be  
95 affected (or intentionally modified) by many factors [17] including temperature, impurities in the  
96 water, as well by the thickness of the water sheet. The efficacy of tap water to absorb the  
97 broadband radiation emitted by a hydrocarbon fire was determined empirically. Exploratory  
98 experiments showed that the radiant energy produced by a natural gas diffusion flame could be  
99 reduced from 100 kW/m<sup>2</sup> to less than 1 kW/m<sup>2</sup> behind a 30 mm thick sheet of tap water. This  
100 insight was first used to protect distance measurement lasers [18] from thermal radiation in ‘dry’  
101 systems, where the measurement instrument was placed behind a moving sheet of water, and  
102 subsequently in ‘wet’ systems with traditional, i.e., not 360-degree, video cameras, where the  
103 camera was placed in the water in a waterproof enclosure. The advantage of a ‘wet’ system over  
104 a ‘dry’ system is that the water serves the dual purpose of cooling the camera.

105 Fig. 4 shows a concept sketch of the extension of the ‘wet’ system to a 360-degree camera. The  
106 design has been implemented with various monoscopic 360-degree cameras, which provide flat,  
107 spherical projections, but could potentially be adapted for use with stereoscopic cameras that also  
108 provide depth information. Several waterproof sports action 360-degree cameras are  
109 commercially available for under 800 USD and products are rapidly getting better, cheaper, and  
110 smaller. The 360-degree camera is placed at the center of a transparent globe made of  
111 temperature-resistant glass. The glass dome is clamped to a pipe flange and made watertight with  
112 a temperature-resistant silicon O-ring. A ceramic fabric gasket is placed between the clamping  
113 ring and the glass dome to reduce stress concentrations and the chance of cracking the dome. The  
114 pipe flange has a diaphragm at its center with two holes and is connected to a threaded pipe. The  
115 holes allow for water to flow into and out of the dome. The outflow hole in the diaphragm is  
116 connected to a flexible tube with a diameter smaller than that of the threaded pipe. A flow  
117 separator divides the lower portion of the glass dome into inflow and outflow sides. Finally, an  
118 air bleed tube runs from the top center of the dome into the outflow tube.



119  
120 Fig. 4. Schematic illustration of 360-degree camera enclosure (image credit: N. Hanacek/NIST).

121 The cool water flowed into the dome cools both the construction and the camera and forces out  
122 the heated water that is absorbing the radiation from the fire. The flow separator causes mixing  
123 of the cool and heated water in the dome. Due to the pressure difference between the water at the  
124 top of the dome and in the outflow tube, the air bleed tube, which terminates just below the

125 diaphragm in the outflow tube, ensures that air bubbles in the water supply line or that form due  
126 to micro-boiling at the inner surface of the glass do not collect at the top of the dome.

127 Because the construction is water cooled, most of the parts can be fabricated from mild steel.  
128 Only the clamping ring and posts are not effectively cooled by the water and must be fabricated  
129 using materials capable of withstanding the high temperatures in a fire. Experience has shown  
130 that it is important to reduce thermally-induced stress gradients in the construction as much as  
131 possible; in particular in the glass dome. The design in Fig. 4 is conceived to minimize ‘thermal  
132 shadowing’ on the glass which would cause stress gradients.

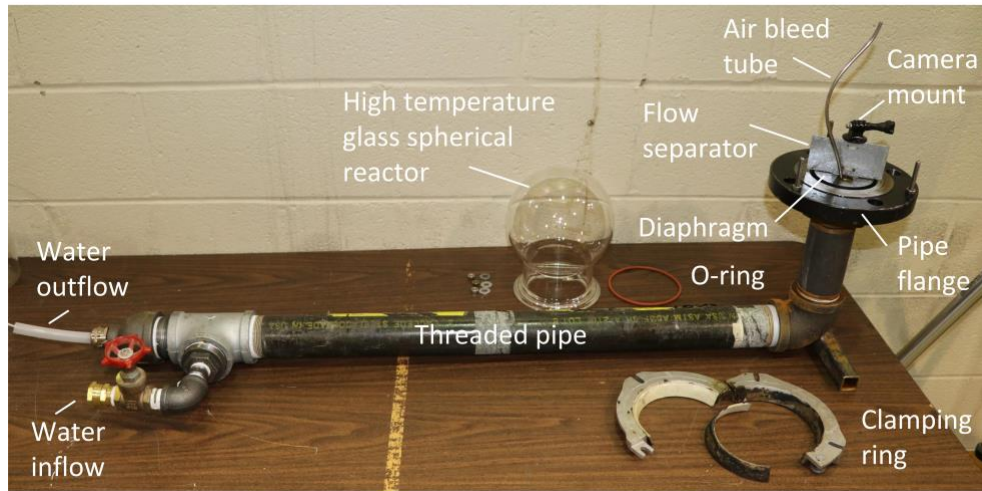
133 Placing the camera in water has two notable drawbacks. First, the camera’s audio fidelity is  
134 significantly reduced, and second, the water changes the index of refraction of visible light which  
135 affects the stitching of the images from the camera. The audio limitation can be overcome in  
136 some applications using external microphones; see Section 4. With regard to the stitching,  
137 monoscopic 360-degree cameras capture video from two cameras with hemispherical lens placed  
138 back-to-back. The video images are stitched together to form a flat spherical image that can be  
139 viewed like a projection on the inside of a globe. Because the water refracts (bends) the visible  
140 light, a portion of the field of view is corrupted along the seam between the two hemispherical  
141 images. This problem could be eliminated using a camera with additional overlapping lens and  
142 more sophisticated stitching techniques. However, the author found that the lost field of view  
143 along the seam (on the order of a few degrees of angle) did not warrant the effort to correct this.  
144 It is noted that scuba divers using 360-degree cameras also face this problem and it is possible  
145 that solutions will be commercially available in the future.

### 146 **3. Fabrication examples**

147 This section provides examples of the fabrication of the above-described concept design. The  
148 detailing and dimensioning of the system can vary based on the fire scenario. The examples  
149 provided are designed for use in large compartment fires or wildland fires.

150 Fig. 5 shows the first functional prototype of what has been named the Burn Observation Bubble,  
151 or BOB for short. Except for the diaphragm, flow separator, and air bleed tube, all of the  
152 components are off-the-shelf items. A spherical reaction vessel made of borosilicate glass that  
153 allows the 360-degree camera to fit through the opening and provides a layer of water in all  
154 directions between the camera and the glass is first selected. Fused silica glass resists higher  
155 temperatures than borosilicate glass and can also be used but is significantly more expensive.  
156 The opening diameter dictates the clamping ring size as well as the pipe flange diameter. In this  
157 prototype a commercial clamping ring for reaction vessels is used to secure the spherical reactor  
158 to the pipe flange. The pipe diameter for the horizontal and vertical portions of the setup is  
159 governed by the magnitude of the thermal energy that will be transferred to the water, the  
160 resulting required volumetric flow rate to transport that heated water out of the setup and replace  
161 it with cool water before exceeding the specified temperature limit of the camera, and the  
162 maximum pressure that the waterproof camera can sustain. By using standard threaded pipe, the  
163 height of the camera and position in a room can be easily varied. The steel diaphragm is drilled  
164 through with two 12 mm diameter holes and welded to a pipe reducer that connects the pipe  
165 flange to the vertical threaded pipe (refer to Fig. 4). The hot water outflow hole is threaded to  
166 allow attachment of a compression fitting for high-density polyethylene tubing that runs inside  
167 the threaded pipe and out the rear of the setup. The flow separator is a thin piece of galvanized

168 sheet steel attached to the camera mount post. Finally, the air bleed tube is constructed from  
 169 stainless steel tube attached to the flow separator.



170

171 Fig. 5. Photograph of first prototype of a Burn Observation Bubble.

172 For the design of the prototype in Fig. 5 it is assumed that a spherical reactor with a radius  $r$  of  
 173 0.0762 m is exposed to a constant heat flux  $q$  of 200 kW/m<sup>2</sup> for an indefinite period of time (i.e.,  
 174 steady state conditions are achieved), that all heat transfer to the water takes place at the  
 175 spherical reactor (i.e., heat transfer to the pipe is neglected), and that an infinite supply of 23 °C  
 176 cooling water is available. The allowable residence time  $t_{res}$  of the water in the spherical reactor  
 177 to not exceed a temperature rise ( $\Delta T$ ) of 20 °C (i.e., a camera temperature of 43 °C) can be  
 178 calculated from the heat capacity as:

179 
$$t_{res} = \frac{\rho \cdot r \cdot c_p \cdot \Delta T}{3 \cdot q} \quad (1)$$

180 where, for water, the density  $\rho$  is 1000 kg/m<sup>3</sup> and the specific heat  $c_p$  is 4200 J/kg-°C. The  
 181 required volumetric flow rate  $\dot{V}$  of water through the sphere of volume  $V$  is then:

182 
$$\dot{V} = \frac{V}{t_{res}} \quad (2)$$

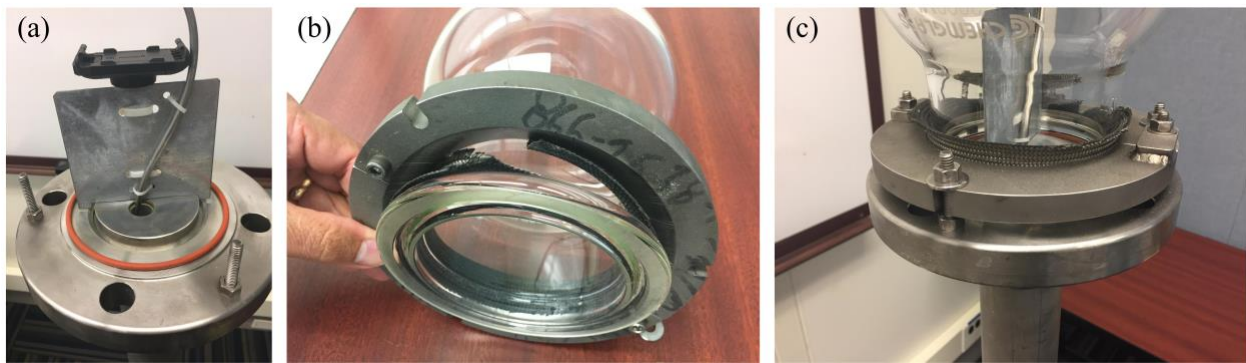
183 For this prototype, this yields an allowable residence time of 10.7 s for the water in the spherical  
 184 reactor and a required volumetric flow rate of the water of  $17.4 \times 10^{-5}$  m<sup>3</sup>/s (10.4 l/min). While  
 185 Eqns. (1) and (2) are often sufficient for design, more detailed heat transfer calculations were  
 186 performed by Yang [19]. Yang's dimensionless solutions based on the energy balance of a  
 187 closed, recirculating system with a heated enclosure and a cooling reservoir incorporate time-  
 188 dependent temperature change of the reservoir and enclosure, as well as the volume ratio of the  
 189 two bodies. While Yang's solutions simplify to Eqns. (1) and (2) under the assumptions stated  
 190 above, in some applications the expanded solutions may be useful for design.

191 The required volumetric flow rate must be supplied with a pressure at the spherical reactor that  
 192 does not exceed the pressure rating of the camera. Pressure to the water inflow in Fig. 5 will vary  
 193 based on factors including on the water supply pressure, as well as the hose diameter and hose  
 194 length between the supply and the setup. Consequently, determining this pressure for a given

195 application using an in-line pressure gauge is recommended. The 50 mm diameter threaded pipe  
196 used for the prototype in Fig. 5 was selected because it provides a stable support for the spherical  
197 reactor and has sufficient inside diameter for the water outflow tube and compression fittings  
198 inside the pipe without restricting the water flow for the design volumetric flow rate.

199 In a setting where enough clean water is available, the cooling water can be supplied by a garden  
200 hose connected to the water supply and the water outflow can be discharged to a drainage. In  
201 humid environments, it is desirable to be able to adjust the inflow water temperature to avoid  
202 condensation from forming on the outside of the glass dome prior to fire growth.

203 Fig. 6 shows details of a subsequent prototype for deployment in wildland fires. In this  
204 application, a recirculated water supply was required so the setup is constructed out of stainless  
205 steel to avoid discoloration of the water due to oxidation. Additionally, the clamping ring (Fig.  
206 6b) is custom made out of Inconel to sustain higher temperatures and the threaded posts and nuts  
207 are made of high-temperature A286 stainless steel (Fig. 6c).



208  
209 Fig. 6. Photographs of a Burn Observation Bubble for field deployment in wildland fires (a) top  
210 of flange without glass dome, (b) glass dome with clamping ring, (c) assembly at pipe flange.

#### 211 4. Application examples

212 The following application examples are selected to illustrate significant evolutions of the system  
213 and learnings from deployments that may be useful to the reader. The 360-degree videos from  
214 these experiments and additional case studies are available online at [https://www.nist.gov/el/fire-  
215 research-division-73300/national-fire-research-laboratory-73306/360-degree-video-fire](https://www.nist.gov/el/fire-research-division-73300/national-fire-research-laboratory-73306/360-degree-video-fire).

##### 216 4.1 Furnished compartment fire

217 An early deployment of the camera system was in a compartment fire inside of a replica of a  
218 museum collection storage room (Fig. 7a). The experiment was part of a training workshop with  
219 the Smithsonian Institution's Preparedness and Response in Collections Emergencies (PRICE)  
220 team held at the National Fire Research Laboratory (NFRL). The fire was ignited using an  
221 'electric match' placed in a trashcan filled with shredded paper and plastic bottles and spread to  
222 involve a cardboard box filled with packing peanuts and neighboring materials (Fig. 7b). The fire  
223 was extinguished manually prior to compartment flashover using an overhead sprinkler when the  
224 upper layer gas temperature in the compartment reached approximately 750 °C. The peak heat  
225 release rate, measured using oxygen consumption calorimetry, was 2350 kW.



226

227 Fig. 7. Furnished compartment fire experiment of a replica of a museum collection storage room:  
228 (a) compartment prior to ignition, (b) fire approximately 4 min after ignition.

229 The 360-degree camera was placed near the center of the room approximately 60 cm up from the  
230 floor. The height and location were selected to provide a good field of view but also so that the  
231 glass dome would stay below the calculated smoke layer. This reduced the chance that the dome  
232 would become obstructed by soot and smoke from the fire. In the approximately half dozen  
233 deployments of the BOB to date, in most cases soot obstruction has been minimal due to  
234 judicious placement of the camera or the use of low soot yield fuels. However, in applications  
235 where the dome becomes engulfed in smoke, soot deposition on the glass will severely limit  
236 visibility, making this setup unsuitable for many compartment fire environments.

237 Using the 360-degree camera setup in this application had three notable advantages over  
238 traditional video cameras. First, a single camera placed near the center of the compartment  
239 allowed viewing of multiple aspects of the experiment, e.g., fire ignition and growth, the  
240 condition of the dummy artifacts (no actual museum objects were used) located throughout the  
241 room, and smoke behavior, that would have otherwise required multiple, thermally-hardened,  
242 video cameras to capture. Second, the video can be viewed using a virtual reality head-mounted  
243 display, which is engaging for communication and training; a key requirement of the  
244 stakeholders from the Smithsonian Institution. Third, it is possible to overlay the resulting 360-  
245 degree video with compartment temperatures measured during the experiment using WebVR  
246 virtual reality software tools. Interactive, data-augmented 360-degree video provides new  
247 possibilities to communicate results from large fire experiments. A disadvantage of this approach  
248 was that, at present, commercially-available waterproof 360-degree video cameras do not permit  
249 wired<sup>1</sup> live streaming of video. This meant that the video was recorded to the local memory on  
250 the camera and viewed after the experiment was complete.

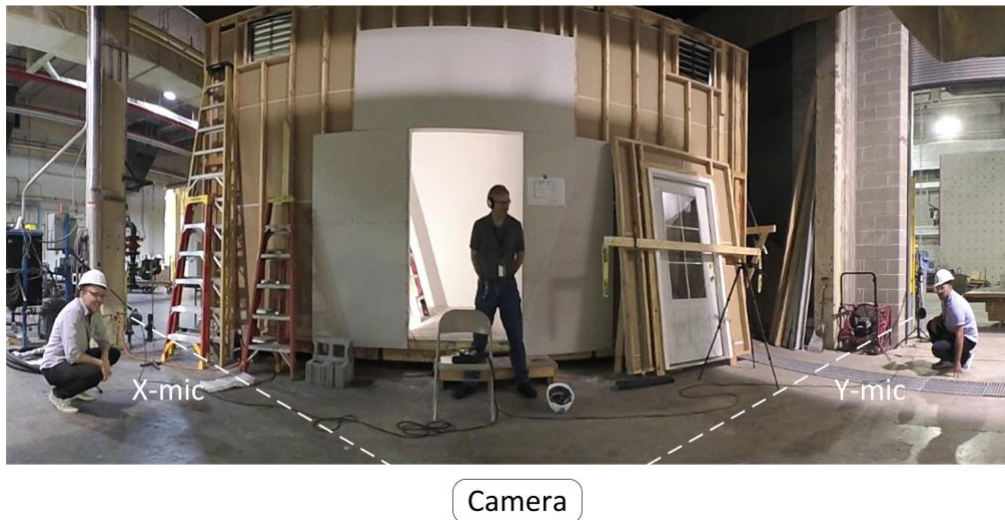
251 During this deployment and a previous one, it was observed that the posts securing the clamping  
252 ring on the first prototype (Fig. 5) underwent excessive thermal expansion which relaxed the seal

---

<sup>1</sup> Wireless live streaming of low-resolution video is possible for many cameras, however, it shortens battery life and wireless communication through water to a receiving device at the standoff distances typically required for large fires is prohibitive.

253 between the glass dome and the pipe flange allowing water to leak. Subsequently, the clamping  
254 ring and posts were redesigned from more temperature resistant materials and the post lengths  
255 were reduced to minimize thermal elongation (refer to Fig. 6).

256 In these experiments external audio was first added. Although audio can be recorded using the  
257 camera's built-in microphones, sounds outside the glass dome are strongly attenuated by the  
258 water. For fires in open areas, audio can be obtained by placing directional microphones, e.g.,  
259 cardioid 'shotgun' microphones, at a sufficient distance from the fire to avoid thermal damage.  
260 By placing two shotgun microphones in an XY-pattern that intersects at the camera (Fig. 8) one  
261 obtains (reversed) stereo sound at the position of the camera. The separately recorded audio can  
262 be overlaid on the video during post-processing. It should be noted that this audio will not track  
263 the rotation of the video during viewing, i.e., if you look 180° from the initial video orientation  
264 the sound will be reversed, however, if additional microphones are used, spatial audio that tracks  
265 the 360-degree field of view can be created using audio post-processing software. High-quality  
266 audio in a fire provides a more immersive viewing experience.

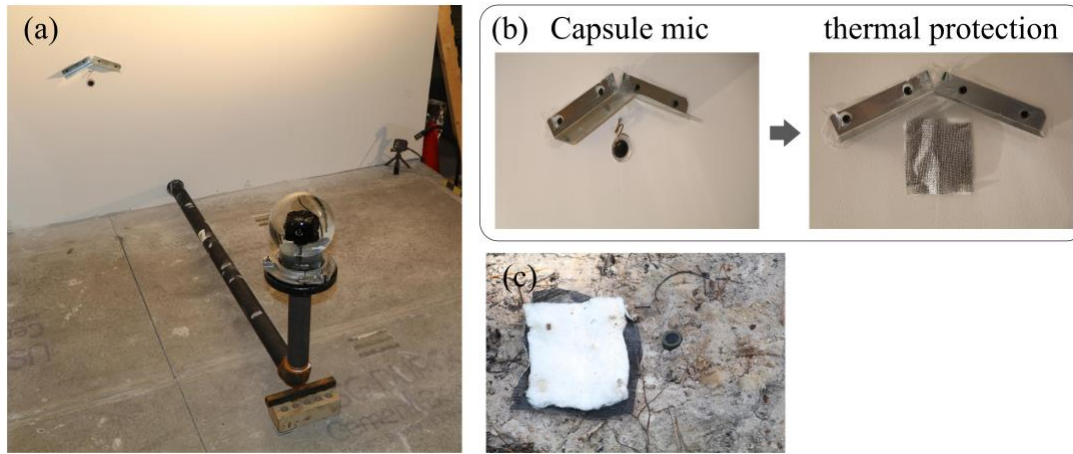


267

268 Fig. 8. Example of directional microphones in an XY-pattern to record audio for fires in an open  
269 area.

270 For enclosed areas like compartment fires, thermally-protected omnidirectional capsule  
271 microphones placed at multiple locations can be used to record audio. An example for the  
272 museum collection fire is shown in Fig. 9a. While there is limited directionality to the audio, i.e.,  
273 sounds close to the mic will sound louder, because the sounds in the room reflect off walls, the  
274 audio still feels natural when overlaid on the 360-degree video. To protect the microphones from  
275 thermal damage, they were placed low on the walls and covered with a noncombustible aramid  
276 fabric and an acoustically-transparent silver scrim to slow convective heat transfer and reflect  
277 radiant energy generated by the fire (Fig. 9b). While this worked for this application,  
278 temperatures measured at the microphones over 100 °C immediately prior to fire suppression  
279 suggest that they would have been destroyed had the fire been allowed to progress to flashover of  
280 the compartment. The sheet metal 'roof' above the microphone in Fig. 9b prevented water from  
281 the sprinklers from running down the wall into the microphone. The same capsule microphones

282 covered with aramid fabric and an acoustically-transparent silver scrim were used to record  
 283 audio successfully in wildland fires, however, in this application the microphones were buried  
 284 underground (Fig. 9c).



285  
 286 Fig. 9. Example of capsule microphones to record audio for fires: (a) one mounting location  
 287 relative to camera in a compartment, (b) detail of thermal protection, (c) capsule microphone  
 288 buried underground for use in wildland fire; the thermal protection is upside down next to  
 289 microphone and not in its final position.

290 **4.2 Prescribed forest management fire**

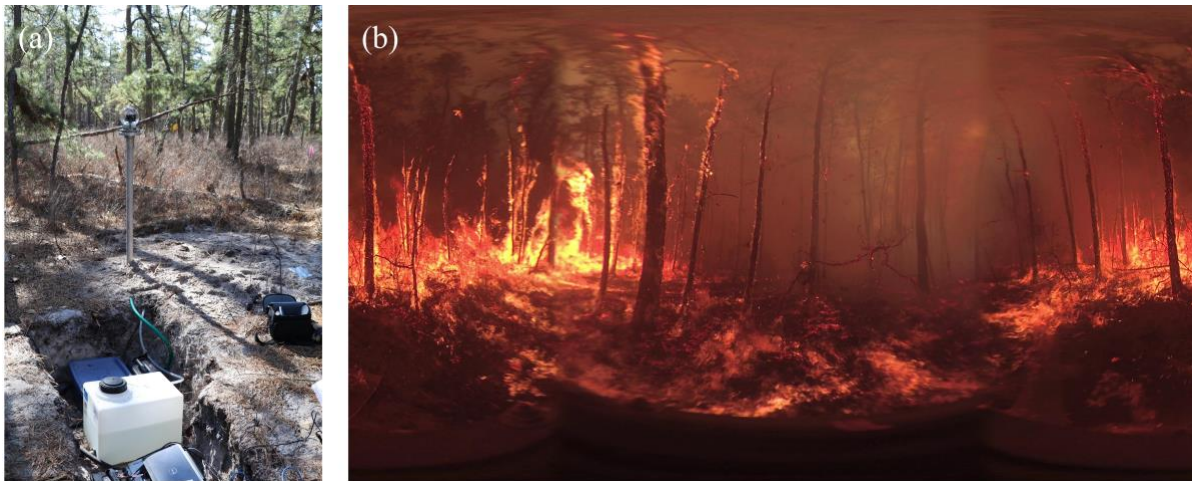
291 360-degree video is particularly well-suited to fires in large areas where the fire moves over  
 292 time. Forest fires are a good example of such an application. The camera system was deployed in  
 293 a series of prescribed forest management fires in the Pinelands National Reserve of New Jersey,  
 294 USA to investigate the performance of the camera system in this application and to provide  
 295 video footage to the U.S. Forest Service and the researchers conducting the burns.

296 Because limited water was available in the forest, a recirculated water-cooling system was  
 297 constructed that consisted of a plastic water tank and battery powered water pump that could run  
 298 for 60 min and be buried underground (Fig. 10a). The required mass of water ( $m_{H2O}$ ) to maintain  
 299 an allowable temperature rise ( $\Delta T$ ) of 20 °C for the camera was estimated assuming that all heat  
 300 transfer from the fire to the water took place at the glass dome according to Eq. (3):

301 
$$m_{H2O} = \frac{q \cdot A \cdot t_{exp}}{c_p \cdot \Delta T} \quad (3)$$

302 where the total heat flux  $q$  at the height of the dome as the fully-developed fire moved past the  
 303 camera was assumed to be 100 kW/m<sup>2</sup>, the surface area of the glass  $A$  was 0.08 m<sup>2</sup>, the exposure  
 304 time  $t_{exp}$  at peak heat flux was assumed to be 10 min, and the specific heat of water  $c_p$  is  
 305 4200 J/kg-°C. This yields a required water mass of 57 kg (57 liters). More detailed heat transfer  
 306 analysis that includes the time-dependent increase in reservoir temperature using the equations  
 307 by Yang [19] show a slightly shorter time of 7 min will result in the 20 °C threshold being  
 308 exceeded under the assumed conditions. Heat transfer to the water through the threaded pipe was  
 309 neglected because it was planned to wrap the pipe in thermal ceramic fiber blanket. Although the  
 310 pipe was ultimately left unwrapped, the above assumptions proved to be suitable for the fires  
 311 studied.

312 360-degree video of two surface fires and one crown fire were recorded. The viewer can watch  
313 the fires progress from when they are lines on the horizon, warp around and engulf the camera  
314 and then recede into the distance. The movement of the treetops caused by the fire-driven winds,  
315 fire spread along the forest floor, as well as ember formation and spotting fires can be viewed in  
316 a single video. This allows the viewer to appreciate the behavior of the fires more completely  
317 than multiple, single camera views, had in past experiments [8]. The video can be unwrapped to  
318 an equirectangular format that allows one to see the fire in all directions at one time (Fig. 10b)  
319 and then zoomed to focus on fire behavior at a specific location of interest.

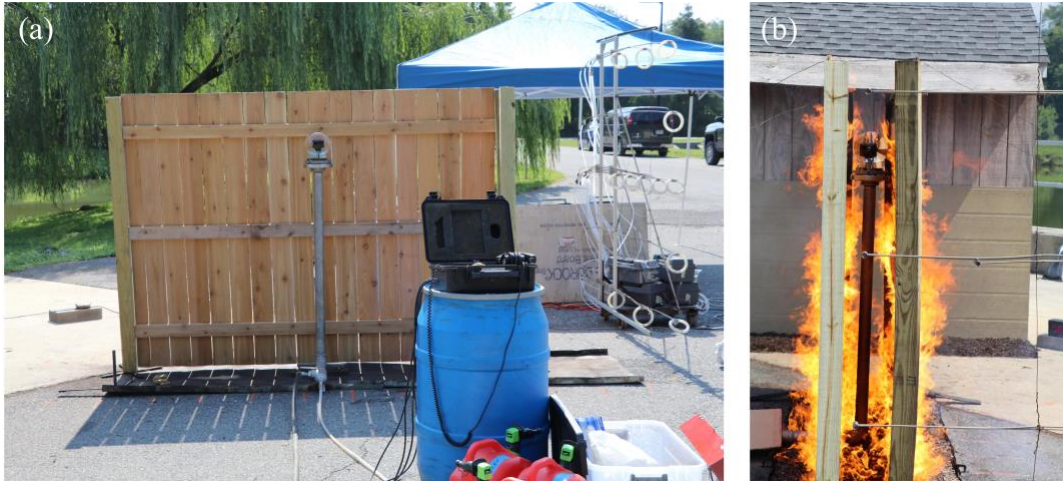


320  
321 Fig. 10. Prescribed forest management fire: (a) camera setup with portable water supply,  
322 (b) equirectangular snapshot from 360-degree video taken during a crown fire.

### 323 4.3 Parallel privacy fence fire

324 The final example is that of a parallel privacy fence fire. Additional information about these  
325 experiments is available in [20]. The camera is placed in close proximity to the burning material;  
326 the fence separation is 30 cm (Fig. 11). This illustrates an example of the camera system in a  
327 well-ventilated confined space with significant thermal radiation. The same recirculating water  
328 system from the prescribed forest management fire discussed above was used. Because the  
329 thermal radiation to the threaded pipe was significant, and not considered in the water mass  
330 calculations, the water exceeded the allowable temperature rise of 20 °C within less than 5 min  
331 and by the end of the approximately 15 min burn duration the water was boiling. While the  
332 camera did not shut down and the video footage was recovered from the memory card following  
333 the experiment, the 360-degree camera was permanently damaged due to water leakage into the  
334 camera.

335 Fig. 12 shows a snapshot of the flame spread along the inside fence surfaces. Without the water  
336 filtering the radiation, a camera could not survive in this intense thermal environment. By  
337 placing a single 360-degree camera at the center of the test specimen, the fire spread along the  
338 inside of the fences can be viewed from a perspective that was previously inaccessible. This is  
339 achieved with limited impact on the air flow between the fences; which was important for the  
340 experiment. Soot deposition was not a problem until late in the fire decay due to the well-  
341 ventilated conditions.



342

343 Fig. 11. Fire test of parallel privacy fence panels: (a) side view of setup prior to placement of  
 344 second fence panel, (b) end view of setup during fire growth.



345

346 Fig. 12. Equirectangular snapshot from 360-degree video taken during parallel privacy fence panel fire.

347 **5. Conclusions and future work**

348 A relatively thin (e.g., 30 mm) layer of water can be used to significantly reduce infrared  
 349 radiation from a fire while remaining transparent to visible light. This insight was used to build  
 350 simple, inexpensive (less than 1000 USD) and robust enclosures for cameras placed in fires. The  
 351 transparent enclosure to house commercial monoscopic 360-degree cameras presented in this  
 352 paper allows users to record video from the middle of intense fires for indefinite durations.

353 The fact that the camera can be placed at the center of a fire, provides new perspectives for many  
 354 applications in fire research. Moreover, by using a 360-degree camera, the viewer can better  
 355 understand the spatial development of the fire or zoom in to focus on specific regions of interest  
 356 that can vary over the duration of the fire.

357 In addition to the video provided by these cameras, which can be viewed in immersive  
 358 environments like the example in Fig. 13, work is ongoing at the National Institute of Standards  
 359 and Technology (NIST) to augment the 360-degree video with measurements taken during fire  
 360 experiments. This data augmented 360-degree video provides the viewer with spatial and

361 temporal context for the measurements and will hopefully be a useful tool for technical  
362 communication in fire science in the future.



363  
364 Fig. 13. 360-degree video taken from within a prescribed forest management fire viewed in a  
365 cave automatic virtual environment (image credit: L. Gerskovic/NIST).

## 366 5. Acknowledgements

367 This work was funded by the National Institute of Standards and Technology. Special thanks are  
368 given to Andrew Mundy, Matthew Bundy, Jeffrey Fagen and Christopher Smith for their support  
369 and expertise, as well as to Michael Gallagher, Rory Hadden, and Erik Johnsson for allowing the  
370 author to deploy the camera in their fire experiments.

## 371 6. References

- 372 [1] A.E. Çetin, K. Dimitropoulos, B. Gouverneur, N. Grammalidis, O. Günay, Y.H.  
373 Habiboğlu, B.U. Töreyn, S. Verstockt, Video fire detection - Review, Digit. Signal  
374 Process. A Rev. J. (2013). doi:10.1016/j.dsp.2013.07.003.
- 375 [2] H. Xiao, M.J. Gollner, E.S. Oran, From fire whirls to blue whirls and combustion with  
376 reduced pollution, Proc. Natl. Acad. Sci. 113 (2016) 9457–9462.  
377 doi:10.1073/pnas.1605860113.
- 378 [3] V.C. Raj, S. V. Prabhu, Measurement of geometric and radiative properties of heptane  
379 pool fires, Fire Saf. J. (2018). doi:10.1016/j.firesaf.2017.12.003.
- 380 [4] J. Fang, J. Wang, R. Tu, R. Shang, Y. ming Zhang, J. jun Wang, Optical thickness of  
381 emissivity for pool fire radiation, Int. J. Therm. Sci. (2018).  
382 doi:10.1016/j.ijthermalsci.2017.10.023.
- 383 [5] L. Bisby, J. Gales, C. Maluk, A contemporary review of large-scale non-standard  
384 structural fire testing, Fire Sci. Rev. 2 (2013) 1–27. doi:10.1186/2193-0414-2-1.
- 385 [6] J.P. Hidalgo, T. Goode, V. Gupta, A. Cowlard, C. Abecassis-Empis, J. Maclean, A.I.  
386 Bartlett, C. Maluk, J.M. Montalvá, A.F. Osorio, J.L. Torero, The Malveira fire test: Full-  
387 scale demonstration of fire modes in open-plan compartments, Fire Saf. J. (2019).  
388 doi:10.1016/j.firesaf.2019.102827.

- 389 [7] T. Beji, S. Verstockt, R. Van de Walle, B. Merci, On the Use of Real-Time Video to  
390 Forecast Fire Growth in Enclosures, *Fire Technol.* 50 (2012) 1021–1040.  
391 doi:10.1007/s10694-012-0262-0.
- 392 [8] J.C. Thomas, E. V. Mueller, S. Santamaria, M. Gallagher, M. El Houssami, A. Filkov, K.  
393 Clark, N. Skowronski, R.M. Hadden, W. Mell, A. Simeoni, Investigation of firebrand  
394 generation from an experimental fire: Development of a reliable data collection  
395 methodology, *Fire Saf. J.* (2017). doi:10.1016/j.firesaf.2017.04.002.
- 396 [9] M.A. Finney, J.D. Cohen, J.M. Forthofer, S.S. McAllister, M.J. Gollner, D.J. Gorham, K.  
397 Saito, N.K. Akafuah, B.A. Adam, J.D. English, Role of buoyant flame dynamics in  
398 wildfire spread., *Proc. Natl. Acad. Sci. U. S. A.* 112 (2015) 9833–8.  
399 doi:10.1073/pnas.1504498112.
- 400 [10] Water cooled camera enclosure for industrial high temperature applications, (n.d.).  
401 [http://www.tecnovideocctv.com/cooled\\_camera\\_enclosure.php](http://www.tecnovideocctv.com/cooled_camera_enclosure.php) (accessed August 28,  
402 2019).
- 403 [11] Videotec Products, (n.d.). [https://www.videotec.com/cat/en/products/fixed-cameras-and-](https://www.videotec.com/cat/en/products/fixed-cameras-and-housings/stainless-steel-housings-and-cameras/nxw/)  
404 [housings/stainless-steel-housings-and-cameras/nxw/](https://www.videotec.com/cat/en/products/fixed-cameras-and-housings/stainless-steel-housings-and-cameras/nxw/) (accessed August 28, 2019).
- 405 [12] D. Madrzykowski, S. Kerber, *Fire Fighting Tactics Under Wind Driven Conditions:*  
406 *Laboratory Experiments*, NIST TN 1618, Gaithersburg, MD, 2009.
- 407 [13] J. Su, P. Lafrance, M. Hoehler, M. Bundy, *Fire Safety Challenges of Tall Wood Buildings*  
408 *– Phase 2: Task 2 & 3 – Cross Laminated Timber Compartment Fire Tests*, Fire Protection  
409 Research Foundation, Quincy, MA, 2018.
- 410 [14] M.S. Hoehler, B. Andres, M.F. Bundy, *Influence of Fire on the Lateral Resistance of*  
411 *Cold-Formed Steel Shear Walls – Phase 2: Oriented Strand Board, Strap Braced, and*  
412 *Gypsum-Sheet Steel Composite (NIST Technical Note 2038)*, Gaithersburg, 2019.  
413 doi:<https://doi.org/10.6028/NIST.TN.2038>.
- 414 [15] A. Putorti, A. Mensch, N. Bryner, G.C.B. Braga, *Thermal Performance of Self-Contained*  
415 *Breathing Apparatus Facepiece Lenses Exposed to Radiant Heat Flux (NIST Technical*  
416 *Note 1785)*, Gaithersburg, MD, 2013. doi:10.6028/NIST.TN.1785.
- 417 [16] M.S. Hoehler, M.F. Bundy, J. Su, *Dataset from Fire Safety Challenges of Tall Wood*  
418 *Buildings – Phase 2: Task 3 - Cross Laminated Timber Compartment Fire Tests*, (2018).  
419 doi:<https://doi.org/10.18434/T4/1422512>.
- 420 [17] M. Chaplin, *Water absorption spectrum*, (2019).  
421 [http://www1.lsbu.ac.uk/water/water\\_vibrational\\_spectrum.html](http://www1.lsbu.ac.uk/water/water_vibrational_spectrum.html) (accessed August 29,  
422 2019).
- 423 [18] M.S. Hoehler, C.M. Smith, *Application of blue laser triangulation sensors for*  
424 *displacement measurement through fire*, *Meas. Sci. Technol.* 27 (2016).  
425 doi:10.1088/0957-0233/27/11/115201.
- 426 [19] J.C. Yang, *On the Cooling of a 360° Video Camera to Observe Fire Dynamics In Situ -*  
427 *NIST TN 2080*, Gaithersburg, MD, 2019. doi:<https://doi.org/10.6028/NIST.TN.2080>.

428 [20] K. Butler; E. Johnsson, Understanding the Fire Hazards from Fences, Mulch, and  
429 Woodpiles, in: Proc. 6th Int. Fire Behav. Fuels Conf., International Association of  
430 Wildland Fire, Missoula, 2019.

431

## 432 **Figure captions**

433 Fig. 1. Snapshot from video footage taken outside of the doorway opening of a fully-developed  
434 furnished compartment fire extracted from [8].

435 Fig. 2. Schematic illustration of relative intensity spectrum of a typical hydrocarbon fire.

436 Fig. 3. Relative transmittance spectrum for 30 mm thick sheet of deionized water.

437 Fig. 4. Schematic illustration of 360-degree camera enclosure (image credit: N. Hanacek/NIST).

438 Fig. 5. Photograph of first prototype of a Burn Observation Bubble.

439 Fig. 6. Photographs of a Burn Observation Bubble for field deployment in wildland fires (a) top  
440 of flange without glass dome, (b) glass dome with clamping ring, (c) assembly at pipe flange.

441 Fig. 7. Furnished compartment fire experiment of a replica of a museum collection storage room:  
442 (a) compartment prior to ignition, (b) fire approximately 4 min after ignition.

443 Fig. 8. Example of directional microphones in an XY-pattern to record audio for fires in an open  
444 area.

445 Fig. 9. Example of capsule microphones to record audio for fires: (a) one mounting location  
446 relative to camera in a compartment, (b) detail of thermal protection, (c) capsule microphone  
447 buried underground for use in wildland fire; the thermal protection is upside down next to mic  
448 and not in its final position.

449 Fig. 10. Prescribed forest management fire: (a) camera setup with portable water supply,  
450 (b) equirectangular snapshot from 360-degree video taken during a crown fire.

451 Fig. 11. Fire test of parallel privacy fence panels: (a) side view of setup prior to placement of  
452 second fence panel, (b) end view of setup during fire growth.

453 Fig. 12. Equirectangular snapshot from 360-video taken during parallel privacy fence panel fire.

454 Fig. 13. 360-degree video taken from within a prescribed forest management fire viewed in a  
455 cave automatic virtual environment (image credit: L. Gerskovic/NIST).

456